GA–A27411

CONTROL AND DISSIPATION OF RUNAWAY ELECTRON BEAMS CREATED DURING RAPID SHUTDOWN EXPERIMENTS IN DIII-D

by
E.M. HOLLMANN, M.E. AUSTIN, J.A. BOEDO, N.H. BROOKS, N. COMMAUX, N.W. EIDIETIS, T.E. EVANS, D.A. HUMPHREYS, V.A. IZZO, A.N. JAMES, T.C. JERNIGAN, A. LOARTE, J. MARTIN-SOLIS, R.A. MOYER, J.M. MUNOZ-BURGOS, P.B. PARKS, D.L. RUDAKOV, E.J. STRAIT, C. TSUI, M.A. VAN ZEELAND, J.C. WESLEY, and J.H. YU

OCTOBER 2012

GENERAL ATOMICS

DISCLAIMER

GA–A27411

CONTROL AND DISSIPATION OF RUNAWAY ELECTRON BEAMS CREATED DURING RAPID SHUTDOWN EXPERIMENTS IN DIII-D

by
E.M. HOLLMANN,* M.E. AUSTIN,† J.A. BOEDO,* N.H. BROOKS, N. COMMAUX,‡
N.W. EIDIETIS, T.E. EVANS, D.A. HUMPHREYS, V.A. IZZO,* A.N. JAMES,#
T.C. JERNIGAN,‡ A. LOARTE,¶ J. MARTIN-SOLIS,§ R.A. MOYER,* J.M. MUNOZ-BURGOS,◊
P.B. PARKS, D.L. RUDAKOV,* E.J. STRAIT, C. TSUI,△ M.A. VAN ZEELAND,
J.C. WESLEY, and J.H. YU*

This is a preprint of a paper to be presented at the Twenty-fourth IAEA Fusion Energy Conf., October 8-13, 2012 in San Diego, California.

*University of California San Diego, San Diego, California.
†University of Texas at Austin, Austin, Texas.
‡Oak Ridge National Laboratory, Oak Ridge, Tennessee.
#Lawrence Livermore National Laboratory, Livermore, California.
¶ITER Organization, St Paul lez Durance, France.
§Universidad Carlos III, Leganés, Spain.
◊Oak Ridge Associated Universities, Oak Ridge, Tennessee.
△Institute for Aerospace Studies, U. of Toronto, Toronto, Canada.

Work supported in part by
the U.S. Department of Energy
under DE-FG02-07ER54917, DE-FG03-97ER54415, DE-FC02-04ER54698,
DE-AC05-00OR22725, DE-AC52-07NA27344, and DE-AC05-06OR23100

GENERAL ATOMICS PROJECT 30200
OCTOBER 2012

Control and Dissipation of Runaway Electron Beams Created During Rapid Shutdown Experiments in DIII-D

E.M. Hollmann 1), M.E. Austin 2), J.A. Boedo 1), N.H. Brooks 3), N. Commaux 4), N.W. Eidietis 3), T.E. Evans 3), D.A. Humphreys 3), V.A. Izzo 1), A.N. James 5), T.C. Jernigan 4), A. Loarte 6), J. Martin-Solis 7), R.A. Moyer 1), J.M. Muñoz-Burgos 8), P.B. Parks 3), D.L. Rudakov 1), E.J. Strait 3), C. Tsui 9), M.A. Van Zeeland 3), J.C. Wesley 3), J.H. Yu 1)

1) University of California San Diego, 9500 Gilman Dr., La Jolla, California 92093-0417, USA
2) University of Texas at Austin, Austin, Texas 78712, USA
3) General Atomics, PO Box 85608, San Diego, California 92186-5608, USA
4) Oak Ridge National Laboratory, PO Box 2008, Oak Ridge, Tennessee 37831, USA
5) Lawrence Livermore National Laboratory, 7000 East Ave, Livermore, California 94550, USA
6) ITER Organization, St Paul Lez Durance 13115, France
7) Universidad Carlos III, Leganés 28911, Spain
8) Oak Ridge Associated Universities, Oak Ridge, Tennessee 37830, USA
9) Institute for Aerospace Studies, University of Toronto, Toronto M5S-1A1, Canada

E-mail contact of main author: ehollmann@ucsd.edu

Abstract. Improvements in runaway electron (RE) beam feedback control in the DIII-D tokamak have enabled stable confinement and ramp down to zero current of RE beams produced in rapid shutdowns. Spectroscopic studies of the RE beams have been used to estimate the RE beam ion and neutral composition, allowing comparison between measured and predicted RE current decay rates. RE current dissipation is shown to be more rapid than expected from avalanche theory. Measurements of the RE energy distribution function have been made, indicating a broad distribution with mean energy of order several MeV and peak energies of order 30–40 MeV. The distribution function appears more skewed toward low energies than expected from avalanche theory, consistent with an anomalous drag/scattering term acting on the REs. The anomalous RE current decay can be enhanced by massive gas injection of additional high-Z impurities into the RE beam. The equilibrium assimilation of these additionally injected impurities appears to be reasonably well described by simple radial pressure balance, which will facilitate evaluation of this technique for ITER.

1. Introduction

Runaway electron (RE) beams occasionally form during disruptions or rapid shutdowns in present tokamaks, and localized wall damage has occurred when these RE beams strike plasma-facing components [1]. In ITER, it is predicted that a large fraction of unmitigated disruptions could lead to high current (multi-MA) RE beams [2]. This is due to the large plasma size (R≈6 m, a≈1.5 m) of ITER, which is expected to lead to smaller prompt loss of RE seeds during the disruption thermal quench (TQ) and larger RE amplification during the current quench (CQ). An uncontrolled multi-MA RE beam-wall strike in ITER could lead to significant localized wall damage [3] and must therefore be avoided. A variety of research has been performed on avoiding instabilities which lead to disruptions, predicting the onset of disruptions, and mitigating unavoidable disruptions in a manner which minimizes the chance of forming a large RE current, either through applied magnetic field errors or through rapid shutdown with massive particle injection [4]. Despite these efforts, the present expectation is that a significant (multi-MA) RE beam will form in many ITER disruptions, even when mitigated, indicating an urgent need for research on safe RE beam dissipation methods.

At this time, it is not certain if the ITER control system will be able to control the position of the RE beam current, since the spatial structure of RE current seeds and the subsequent evolution of RE current are not well known. Present simulations indicate that post-disruption RE beams will drift vertically in ITER, but that this vertical motion may be brought under control for sufficiently large RE beams (>10 MA) [5]. However, since uncontrolled RE beam-wall strikes with currents >2 MA are thought to be potentially intolerable in ITER [6], a method for rapidly reducing current in 2 MA < I_p < 10 MA RE beams may be necessary. In this paper, dissipation of RE beam current with massive high-Z gas injection is investigated. To evaluate the effectiveness of massive high-Z gas injection for RE beam current dissipation in ITER, it is important to understand how the RE beam forms during disruptions and what sets its energy and current profile. Additionally, it is important to understand the assimilation of impurities injected into the RE beam and the processes by which the injected impurities dissipate RE current.

2. Overview of Results

The experiments described here are performed in the DIII-D tokamak [7]. In each experiment, an initially stable discharge is shut down (usually at time t = 2000 ms) with high velocity (v ~ 500 m/s) injection of a single small diameter (D≈2.7 mm) solid argon pellet. In most cases, low elongation (κ≈1.3–1.4), inner wall-limited (IWL), electron cyclotron heated (ECH) target plasmas are used, as these are found to be best for reliably producing large (I_p ≈ 200–400 kA) RE beams.

Two main classes of experiments have been performed on these RE beams, or "RE plateau" plasmas: RE control experiments, where external coils are used to manipulate the RE beam current and position and measure its structure carefully; and RE dissipation experiments, where massive gas injection (MGI) is used to deliver large quantities of gas to the RE beam to collisionally dissipate its current.

In the RE control experiments, it was initially found that the RE beam tends to limit against the center post and then drift vertically to be lost in an uncontrolled fashion against the upper or lower divertor. Subsequently, an open loop outward push from the plasma shaping coils was used to give some radial control, avoiding erratic feedback and avoiding loss of the RE beam into the center post. Finally, robust linear position estimators were implemented to enable vertical control of the RE beam position. With effective vertical position control of the RE beam, ohmic feedback control of the RE beam was demonstrated, as shown in Fig. 1(a), where different RE beams are either held at constant current for 600 ms (blue), or held for 200 ms and then ramped down (red), or immediately ramped to nearly zero current (black) [8].

In the RE dissipation experiments, a vertically stable, current-controlled RE beam [such as the blue curve in Fig. 1(a)] is struck with MGI (typically 300 to 1000 torr-l of neon or argon). An enhanced RE current dissipation rate is frequently observed, as seen in Fig. 1(b). The enhanced current decay seen following high-Z MGI occurs despite the ohmic coil ("E-coil") loop voltage attempting to hold the plasma current constant; the resulting decay

rate is similar to that observed if a plasma without MGI is ramped down to zero as rapidly as possible with the E-coil, Fig. 1(a).

3. RE Beam Structure

Understanding the spatial structure of the RE beams is necessary for interpreting line-integrated spectroscopy data for estimating RE beam ion composition and comparing measured RE current decay rates with theory. The spatial structure of RE beams is deduced from two types of inversions: (a) inversions of soft x-ray (SXR) and interferometer data are performed on fast downward-moving plasmas not using magnetic flux contours to demonstrate that both hot and cold electron densities are reasonably approximated by magnetic flux contours (Sec. 3.1); and then (b) inversions of line-integrated spectrometer data using magnetic flux contours are performed on stationary plasmas in order to demonstrate that neutrals are largely excluded from the RE beam core (Sec. 3.2). The energy spectrum of the RE beam fast electrons is reconstructed by combining SXR, HXR, and visible synchrotron emission data (Sec. 3.3).

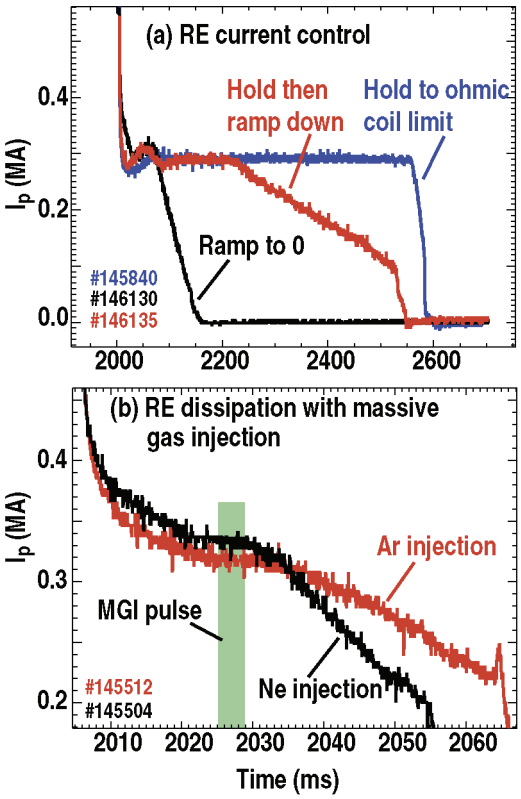

FIG. 1. (a) Runaway electron beam current control showing: shot with constant current out to ohmic coil limit, shot held for 200 ms then ramped down, and shot immediately ramped down to zero current; (b) Dissipation of runaway electron beam current following massive gas injection of 320 torr-l argon or 1050 torr-l neon.

3.1. Hot and cold electron radial profiles

Inversions of downward-moving plasmas for two similar shots are shown in Fig. 2. The total electron density consists of two components: a cold, dense background plasma and a hot, low density RE beam component. The line-integrated cold background plasma electron density can be measured with CO_2 interferometers, and the line-integrated hot electron density can be estimated from SXR view chords. Figure 2(a) shows SXR view chords and magnetic flux surface reconstructions during downward motion. The flux surfaces are calculated with a discrete current element inversion code (JFIT) constrained by external magnetic sensors [9]. Figure 2(b) shows measured SXR brightness vs channel number for three different time steps, as well as back-constructed SXR brightness from the inversion, showing a reasonably good fit. Figure 2(c) shows SXR emissivity contours and JFIT contours. Typically, we find that the SXR center and the JFIT center are within <10 cm of each other. Figure 2(d–f) shows the reconstructed cold electron density profile for a similar but different discharge; it can be seen that the cold electron profile [Fig. 2(f)] is much broader than the hot electron density profile [Fig. 2(c)].

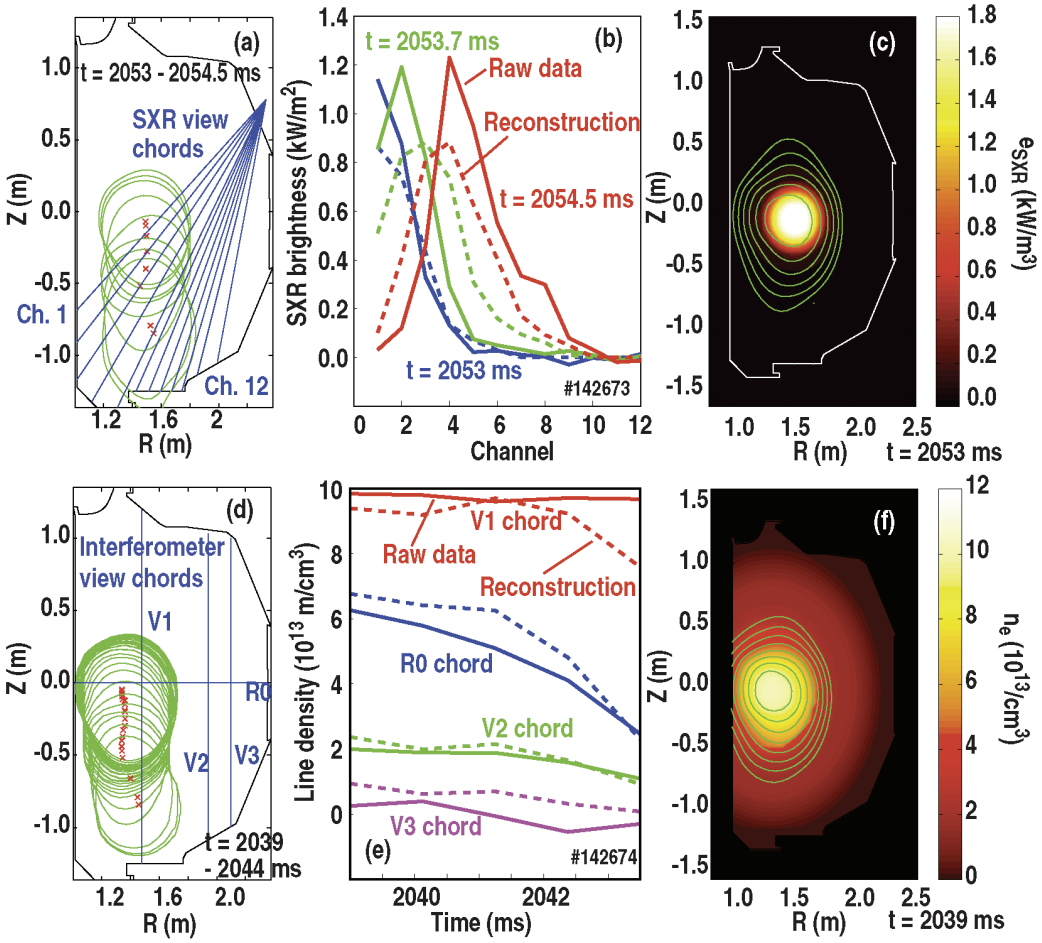

FIG. 2. SXR inversion showing: (a) JFIT reconstructions of flux surfaces of downward moving RE beam, (b) SXR brightness vs array channel number at different time steps, and (c) reconstructed SXR emissivity and JFIT flux surfaces; interferometer inversion showing: (d) JFIT reconstructions of flux surfaces, (e) line-integrated data vs time, and (f) reconstructed cold electron density contours.

3.2. Neutral atom radial profiles

Tangential visible camera images suggest that visible line emissivity is a reasonably good flux function [10]. Using JFIT contours as line emissivity contours, it is possible to use line-integrated visible line brightness data from stationary RE plateau plasmas to make estimates of the ion and neutral densities in the RE beam. Deuterium density can be estimated from D_α (656.2 nm) brightness, Ar^+ density from Ar-II (465.8 nm) brightness, Ar density from Ar-I (811.5 nm) brightness, and C^+ density from C-II (657.8 nm) brightness. Photon emission coefficients from ADAS [11] are used. The D^+ density can then be estimated from quasi-neutrality using the interferometer data. Figure 3 shows the resulting profiles for (a) D and D^+ and (b) Ar and Ar^+. The quality of the reconstructed line-integrated data is shown in panes (c) for interferometer data, (d) for Ar-I brightness, (e) for Ar-II brightness, and (f) for D_α brightness. Due to the small radial shift observed in the SXR inversions, these inversions allow for a small (<10 cm) radial shift of the flux function contours to allow the best possible fit. Overall, it can be seen that the data is fitted within a factor of two or better across the plasma profile. Neutrals are seen to be mostly excluded from the RE beam core. C^+ density, not shown here, is found to be small (~1%) in the RE beam core.

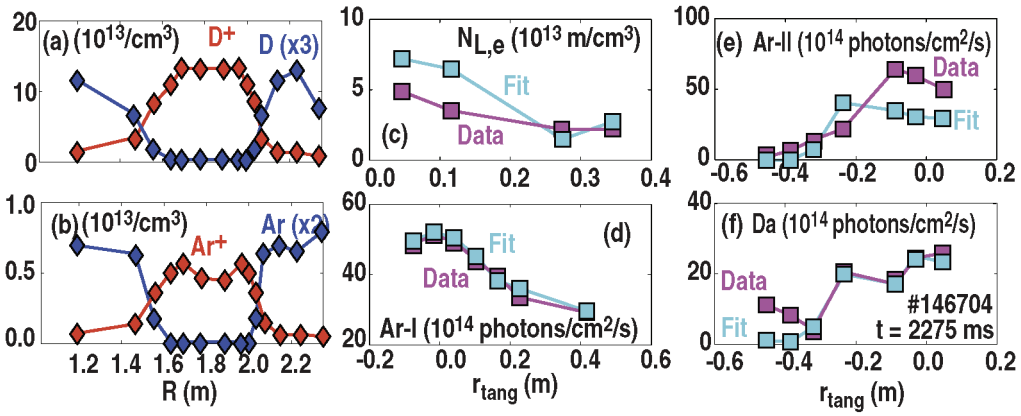

FIG. 3. Midplane density profiles at t = 2275 ms for (a) deuterium neutrals and ions and (b) argon neutrals and ions as a function of midplane radius. (c–f) show quality of fits to line-integrated electron density and line brightnesses. r_{tang} is distance of closest approach of view chord to magnetic axis, with negative values indicating view chord passes between magnetic axis and center post.

For the fits shown in Fig. 3(c–f), the radial electron temperature profile was varied as a free parameter. Central electron temperatures of about 1.4–1.8 eV and edge temperatures of about 0.8–1.4 eV are obtained. These are roughly consistent with measured line widths of about 1.6 eV for ions and 1.2 eV for neutrals [10]. This suggests that the visible line emission is dominated by cold electron collisions, not hot electron collisions, i.e. the interaction between the cold electrons and ions is stronger than the interaction between hot electrons and ions.

3.3. Fast electron energy distribution

An estimate of the RE energy distribution function $f_{RE}(\varepsilon)$ can be assembled from different diagnostics, each dominantly sensitive to a different part of the RE energy distribution: Si SXR detectors (mostly sensitive to electrons in the 2–20 keV range), perpendicular-viewing BGO hard x-ray (HXR) detectors (mostly sensitive to electrons in the 1–5 MeV range), parallel-viewing HXR detectors (mostly sensitive to electrons in the 2–20 MeV range), and visible synchrotron emission (mostly sensitive to electrons in the 30+ MeV range).

Figure 4(a) shows an example of a single-energy fit to the measured visible synchrotron emission spectrum. Single-energy fits can be used to construct a rough $f_{RE}(\varepsilon)$, as shown by the circles and error bars in Fig. 4(b). An improved $f_{RE}(\varepsilon)$ can be obtained by doing a self-consistent fit to all the diagnostics, shown by the red curve in Fig. 4(b). Expected x-ray brightnesses are calculated using the bremsstrahlung simulations of Ref. 12.

The HXR and synchrotron emission signals are sensitive to the RE pitch angle θ, but the SXR brightness is not, so the fit to $f_{RE}(\varepsilon)$ of Fig. 4(b) is insensitive to the value of θ at low energies and a single pitch angle fit, giving $\theta \approx 0.2$, is used. Integrating over $\int dA \int d\varepsilon f_{RE}(\varepsilon) v$ in Fig. 4(b) gives a plasma current which is much larger than observed. If instead, it is assumed that only REs with some minimum energy, ε_x, carry current, then the normalization to plasma current gives $\varepsilon_x \approx 100$ keV, suggesting that low energy electrons are less directional and have a higher pitch angle. Electron cyclotron emission (ECE) is very sensitive to RE pitch angle. The measured RE ECE spectrum from radiometers and a Michelson interferometer is shown

by points in Fig. 4(c). The curves are predicted spectra for different assumptions of the pitch angle θ. It can be seen that the data is reasonably well fitted using the measured distribution function $f_{RE}(\varepsilon)$ and assuming a large pitch angle θ=0.8 for energies ε<100 keV and small pitch angle θ=0.2 for energies ε>100 keV. The model curves in Fig. 4(c) are calculated using the Schott-Trubnikov formula for single particle x-mode ECE [13]. Collective effects are ignored, so these curves are not expected to be valid in the shaded cutoff region of Fig. 4(c).

The dashed line in Fig. 4(b) is the distribution function expected from avalanche theory, $f_{RE}(p) \sim exp(-p/m_e c\,\bar{p})$, with $p \equiv m_e c\beta\gamma$ and $\bar{p} \equiv [3(Z+5)/\pi]^{1/2}\, ln[\Lambda(Z)] \approx 46$ for argon [14]; the normalization is obtained from the plasma current, assuming all plasma current is carried by the fast electrons. It can be seen that the measured distribution function appears skewed toward low energies, possibly indicating an anomalous collisional drag on the fast electrons.

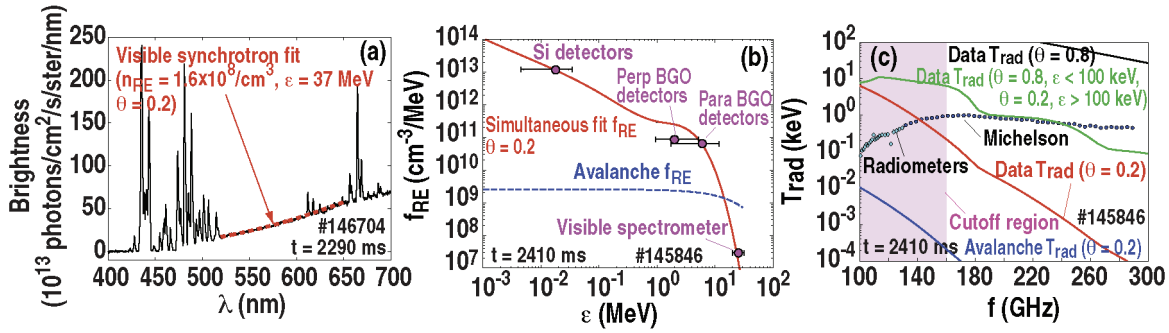

FIG. 4. Estimates of RE energy/pitch angle distribution from: (a) single-energy fit to visible synchroton emission, (b) single-energy fits to SXR, HXR, and visible synchrotron emission (circles) as well as self-consistent fit to all diagnostics simultaneously (red curve); and (c) fits to ECE emission spectrum.

4. Dissipation of RE Current With MGI

As shown in Fig. 1(b), MGI of high-Z gas into RE beams can overcome E-coil feedback control of the RE current and cause a decay of the RE current. Equilibrium assimilation of atoms injected either as gas (MGI) or large frozen pellets [shattered pellet injection (SPI)] into RE beams appears to be fairly low, of order several percent, as shown in Fig. 5. Radial pressure balance gives an expected assimilation fraction $f_{Assim} \approx (V_{beam}/V_{vac})(T_N/T_i)$, where $(V_{beam}/V_{vac}) \approx 1/30$ is the beam/vacuum chamber volume ratio, and $T_{ratio} = (T_N/T_i)$ is the neutral/ion temperature ratio. The high-Z injection data appears consistent with the temperature ratio $T_{ratio} \approx 1/2$ measured for

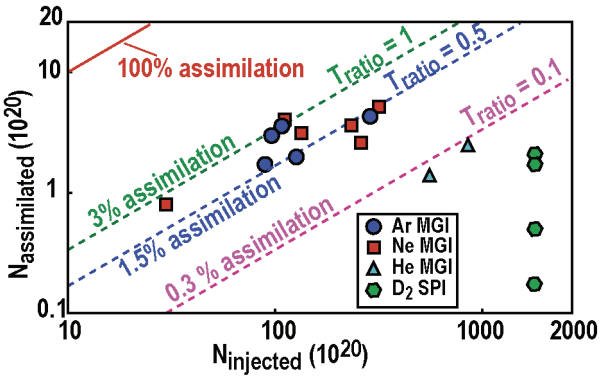

FIG. 5. Assimilation of atoms injected into RE beam showing number assimilated as a function of number injected. Dashed lines show assimilation expected from radial pressure balance assuming different temperature ratios T_{ratio} of RE beam core (ion) temperature over RE beam edge (neutral) temperature.

equilibrium (no MGI) RE beams, however, the lower assimilation of low-Z atoms appears more consistent with a lower temperature ratio $T_{ratio}\approx 1/10$.

The decay of RE current observed in these experiments is qualitatively in agreement with avalanche theory but requires the addition of an anomalous loss term in nearly all cases. According to avalanche theory [15], the growth/decay of RE current is given by $\nu_R = C(E - E_{crit})$, where C is effectively a constant, $\nu_R = J_{RE}^{-1} dJ_{RE}/dt$ is the decay rate of RE current, E is the toroidal electric field, and $E_{crit} \propto n_{e,tot}$ is the critical field for RE suppression. Comparison with this theory is made in two cases: E-coil ramp experiments where the toroidal electric field is changed by the E-coil, resulting in a ramp up or down of the RE current; and MGI experiments, where the E-coil is used in current feedback mode (attempting to maintain the RE current constant) but a large quantity of impurities is injected into the RE beam. In the E-coil ramp experiments, the magnitude of E tends to be large compared with E_{crit}~0.1 V/m, while in the MGI experiments, E_{crit} can be significant in some cases (of order 0.5 V/m or larger). The toroidal electric field E on center of the RE beam is estimated from the time evolution of the magnetic flux obtained from JFIT inversions, averaged over the RE beam radius. As discussed previously [10], E on center of the beam can be calculated from E measured at the edge of the tokamak for a steady RE beam; but in the MGI experiments, the RE beam position and profile are frequently evolving in time, so the JFIT inversions are used here. Figure 6 shows ν_R as a function of $E - E_{crit}$ for (a) E-coil ramp experiments (with the comparison taken in the middle of the RE plateau) and (b) MGI experiments (with the comparison taken as late as possible in the RE plateau before the final RE loss, in order to allow time for toroidal symmetrization of injected impurities). It can be seen that the measured decay rate tends to be 10/s to 20/s lower than expected from avalanche theory. There is some preliminary suggestion in Fig. 6(b) that this anomalous loss of RE current is due to high-Z impurities — this is seen in the low-Z injection experiments, which appear to give RE current decay rates in better agreement with theory, as highlighted with the oval in Fig. 6(b). A possible source of the anomalous loss could be pitch-angle scattering of fast electrons off high-Z nuclei, which is ignored in present avalanche theory.

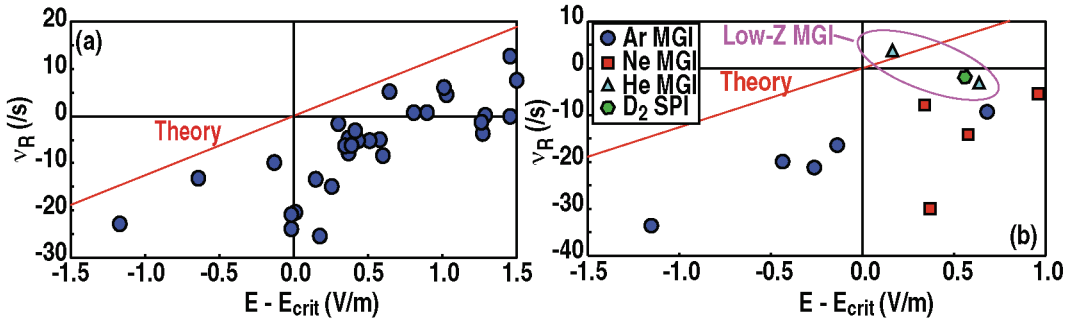

FIG. 6. RE current decay rate ν_R as a function of toroidal electric field E minus critical field E_{crit} in (a) experiments where E is ramped up or down using the E-coil and (b) experiments where the E-coil is attempting to hold I_p fixed, and massive particle injection is used to cause RE current decay.

5. Summary

We have shown that the REs in the RE plateau phase are dominantly confined to a narrow (a≈0.2–0.3 m) near-circular beam. Neutral density appears to be large in most of the vacuum vessel, but smaller inside the RE beam. The energy distribution function of the REs appears to be quite broad, with a mean energy of around 1 MeV, but extending up to energies ε>30 MeV. The distribution function appears to be more skewed toward low energies than predicted by avalanche theory. The plasma current appears to be carried mostly by REs with energies $\varepsilon \geq 100$ keV and low pitch angle $\theta \approx 0.2$, while electrons with energy ε<100 keV appear to have larger pitch angle and carry less current. Dissipation of RE current appears to follow the expected trend with toroidal electric field from avalanche theory, but with an added anomalous loss rate of about 10/s–20/s; comparison of data from low-Z and high-Z massive gas injection experiments suggests that this anomalous loss may be associated with the presence of high-Z nuclei (argon) in the RE beam. Assimilation of gas injected into the RE beam appears to be low, of order several percent, consistent with radial pressure balance. Despite this low assimilation, achieving fairly rapid (~50 ms timescale) ramp down of RE beam current with massive high-Z gas injection appears relatively straightforward, suggesting that this method may be useful for RE beam dissipation in ITER.

This work was supported in part by the US Department of Energy under DE-FG02-07ER54917, DE-FG03-97ER54415, DE-FC02-04ER54698, DE-AC05-00OR22725, DE-AC52-07NA27344, and DE-AC05-06OR23100.

References

[1] NYGREN, R., et al., J. Nucl. Mater. **241** (1997) 522.
[2] HENDER, T.C., et al., Nucl. Fusion **47** (2007) S128.
[3] SIZYUK, V., et al., Nucl. Fusion **49** (2009) 095003.
[4] HOLLMANN, E.M., et al., J. Nucl. Mater. **415** (2011) S27.
[5] PUTVINSKI, S., "Runaway electrons in tokamaks and their mitigation in ITER," presented at US-BPO Disruptions Workshop, San Diego (2012).
[6] LOARTE, A., et al., Nucl. Fusion **51** (2011) 073004.
[7] LUXON, J.L., Nucl. Fusion **42** (2002) 614.
[8] EIDIETIS, N.W., et al., Phys. Plasmas **19** (2012) 056109.
[9] HUMPHREYS, D.A., et al., Phys. Plasmas **13** (2006) 056113.
[10] HOLLMANN, E.M., et al., Nucl. Fusion **51** (2011) 103026.
[11] SOMMERS, H.P., et al., Plasma Phys. Controlled Fusion **44** (2002) B323.
[12] SELTZER, S.M., et al., Nucl. Instrum. Methods B **12** (1985) 95.
[13] CELATA, C.M., et al., Nucl. Fusion **17** (1977) 4.
[14] PARKS, P.B., et al., Phys. Plasmas **6** (1999) 2523.
[15] ROSENBLUTH, M.N., et al., Nucl. Fusion **37** (1997) 1355.